Direct finite element method for nonlinear analysis of semi-unbounded dam-water-foundation rock systems

Arnkjell Løkke[1] and Anil K. Chopra[2]

[1] Department of Structural Engineering, Norwegian University of Science and Technology, 7491 Trondheim, Norway.

[2] Department of Civil and Environmental Engineering, University of California Berkeley, Berkeley, CA 94720, U.S.A.

DISCLAIMER

SUMMARY

A direct finite element method is presented for nonlinear earthquake analysis of interacting dam-water-foundation rock systems. The analysis procedure applies viscous damper absorbing boundaries to truncate the semi-unbounded fluid and foundation-rock domains, and specifies at these boundaries effective earthquake forces determined from the design ground motion defined at a control point on the free surface. The analysis procedure is validated numerically by computing the frequency response functions and transient response of an idealized dam-water-foundation rock system and comparing against results from the substructure method. Because the analysis procedure is applicable to nonlinear systems, it allows for modeling of concrete cracking, as well as sliding and separation at construction joints, lift joints, and at concrete-rock interfaces. Implementation of the procedure is facilitated by commercial finite element software with nonlinear material models that permit modeling of viscous damper boundaries and specification of effective earthquake forces at these boundaries.

1. INTRODUCTION

Evaluating the seismic performance of concrete dams requires dynamic analysis of two- or three-dimensional dam-water-foundation rock systems that recognize the factors known to be significant in the earthquake response of dams [1]: dam-water interaction including water compressibility and wave absorption due to sediments at the reservoir bottom [2,3]; dam-foundation rock interaction including inertia effects of the rock [3,4]; radiation damping due to

the semi-unbounded sizes of the reservoir and foundation-rock domains [4,5]; spatial variation of ground motion [6]; nonlinear behavior of the dam and foundation rock [7–11].

Analysis procedures based on the *substructure method* have been available since 1984 for frequency-domain analysis of the dam-water-foundation rock system [12,13]. These procedures model the semi-unbounded domains rigorously and specify the ground motion directly at the dam-foundation rock interface; however, they are restricted to homogeneous material properties and simple geometry of the reservoir and foundation-rock domains. More importantly, the substructure method is restricted to linear behavior of the entire system. Thus, nonlinear effects such as concrete cracking and separation and sliding at joints and interfaces cannot be modeled.

The *direct method* of analysis on the other hand, models the entire system in the time-domain using finite elements. For many years, the dam engineering profession used a FE model that included a limited extent of foundation rock, assumed to have no mass, and approximated hydrodynamic effects by an added mass of water moving with the dam. The design ground motion – typically defined at a control point on the free surface – was applied at the bottom fixed boundary of the foundation-rock domain. These approximations are attractive because they simplify the analysis greatly, however, such a model solves a problem that is very different from the real problem on two counts: (1) the assumptions of massless rock and incompressible water – implied by the added mass water model – are unrealistic, as research has demonstrated [1]; and (2) applying ground motion specified at a control point on the free surface to the bottom boundary of the FE model contradicts recorded evidence that motions at depth generally differ significantly from surface motions. In recent years, some engineers have shifted away from this approach [14,15].

To eliminate these unrealistic assumptions, the FE model of the dam must be extended to comprise a foundation-rock domain that includes mass, stiffness, and material damping appropriate for rock, and a fluid domain that includes water compressibility and reservoir bottom sediments. The semi-unbounded foundation-rock and fluid domains must be reduced to bounded sizes with appropriate radiation conditions at the domain boundaries to allow propagation of outgoing waves. Development of such *absorbing boundaries* is a vast field with rich literature [16–18]. The earthquake motion cannot be specified directly at the model truncations as this would render any absorbing boundary ineffective. Instead, *effective earthquake forces* are computed from the earthquake excitation and applied either directly at the absorbing boundaries [19–21] or via a single layer of finite elements interior of the absorbing boundaries [22–24].

Utilizing these concepts, a direct finite-element procedure for nonlinear analysis of dam-water-foundation rock systems was developed by Basu [25]. Here, the high performing Perfectly Matched Layer (PML) [26] was selected as the absorbing boundary, and the Effective Seismic Input (ESI) method [22], also known as the Domain Reduction Method (DRM) [24], was used to determine the effective earthquake forces. Although the procedure rigorously incorporates all the previously stated factors significant in the earthquake response of dams, the PML boundary and DRM procedure are currently not available in most commercial FE codes; the only exception is LS-DYNA [27]. Thus, this procedure is not accessible to researchers and practicing engineers who, for various reasons, prefer other FE codes. These limitations can be overcome by modeling the absorbing boundaries by viscous dampers [28] and specifying the effective earthquake forces directly at these boundaries. Both of these features are available in most commercial FE codes and are therefore chosen herein.

The objective of this paper is to develop a direct finite element method for nonlinear analysis of semi-unbounded dam-water-foundation rock systems that incorporates all factors

significant in the earthquake response of dams, while ensuring broad applicability by using the well-known viscous dampers as absorbing boundaries. The equations of motion for the combined dam-water-foundation rock system are derived, and the analysis procedure is validated by computing the dynamic response of an idealized dam-water-foundation rock system and comparing against results from the substructure method.

2. SYSTEM AND GROUND MOTION

2.1. Semi-unbounded dam-water-foundation rock system

The idealized, two-dimensional dam-water-foundation rock system (Fig. 1) consists of three components: (1) the dam with nonlinear properties; (2) the foundation-rock domain, consisting of a bounded region adjacent to the dam that may be nonlinear and inhomogeneous, and a semi-unbounded region that is restricted to be linear; and (3) the fluid domain, consisting of a bounded region of arbitrary geometry adjacent to the dam that may be nonlinear, and a prismatic channel, unbounded in the upstream direction, that is restricted to be linear. Thus, nonlinear effects such as concrete cracking, sliding and separation at construction joints, lift joints, and concrete-rock interfaces, and cavitation in the fluid may be considered in the analysis.

The earthquake excitation is defined at a control point at the surface of the foundation rock by two components of free-field ground acceleration (Fig. 1): the horizontal component $a_g^x(t)$ transverse to the dam axis, and the vertical component $a_g^y(t)$. The surface of the foundation-rock is assumed to be at the same elevation in the far upstream and downstream directions; this geometric restriction is introduced to define a convenient free-field state of the foundation rock in Section 3.

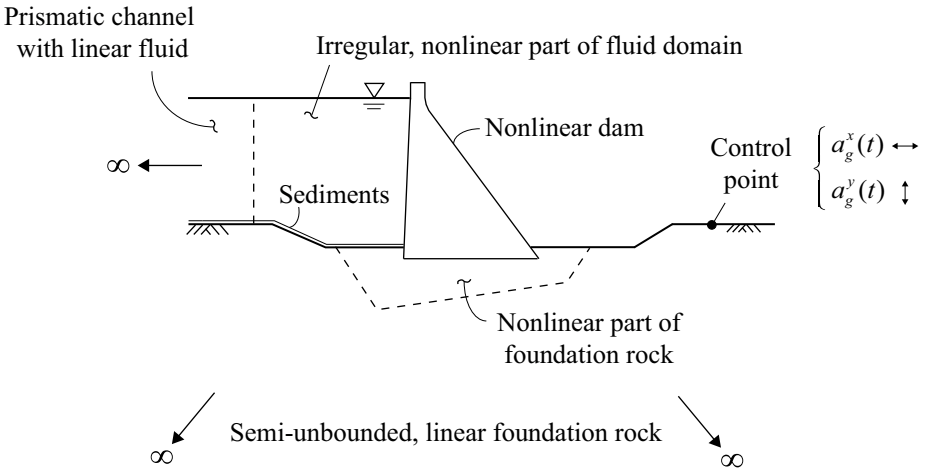

Figure 1. Semi-unbounded dam-water-foundation rock system showing main components: (1) the dam itself; (2) the foundation rock, consisting of a bounded, nonlinear region and a semi-unbounded, linear region; and (3) the fluid domain, consisting of an irregular, nonlinear region, and a semi-unbounded prismatic channel with linear fluid.

The dam-water-foundation rock system in Fig. 1 will be modeled by a finite-element discretization of a bounded system with viscous damper boundaries to represent the semi-unbounded foundation-rock and fluid domains. The size of the foundation-rock and fluid domains included in this FE model is determined by the ability of the absorbing boundaries to absorb outgoing (scattered) waves from the dam. If an advanced boundary such as the PML is used, a small domain is sufficient to model the fluid and foundation-rock domains (Fig. 2a). In contrast, the simple viscous damper boundary selected in this formulation requires much larger domains (Fig. 2b).

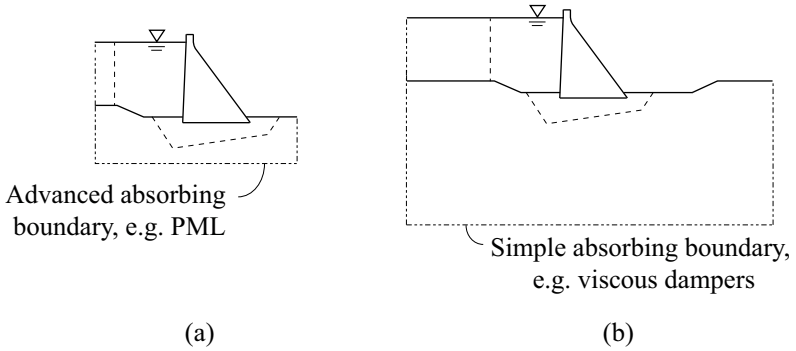

Figure 2. Dam-water-foundation rock system with truncated foundation-rock and fluid domains: (a) small domain sizes with advanced absorbing boundary; (b) large domain sizes with simple absorbing boundary.

2.2. Governing equations

2.2.1. Dam and foundation-rock domain

The equations of motion governing the vector of total displacements $\mathbf{r}^t$ of the finite-element model for the dam with a truncated foundation-rock domain and absorbing boundary Γ_f (Fig. 3) are

$$\mathbf{m}\ddot{\mathbf{r}}^t + \mathbf{c}\dot{\mathbf{r}}^t + \mathbf{f}(\mathbf{r}^t) = \mathbf{R}_h^t + \mathbf{R}_b^t + \mathbf{R}_f^t + \mathbf{R}^{\mathrm{st}} \tag{1}$$

where $\mathbf{m}$ and $\mathbf{c}$ are the mass and damping matrices, respectively; $\mathbf{f}(\mathbf{r}^t)$ is the vector of internal forces due to material response, which may be nonlinear in the dam and adjacent part of the foundation rock; $\mathbf{R}_h^t$ and $\mathbf{R}_b^t$ are the vectors of hydrodynamic forces acting at the dam-water interface Γ_h and water-foundation rock interface Γ_b, respectively; $\mathbf{R}^{\mathrm{st}}$ is the vector of static forces, including self-weight, hydrostatic pressures, and static foundation-rock reactions at Γ_f; and $\mathbf{R}_f^t$ are the dynamic forces associated with the absorbing boundary Γ_f, which includes the effect of the excitation caused by seismic waves propagating from a distant earthquake source to the dam site, and the radiation condition at the boundary. Expressions for the forces $\mathbf{R}_h^t$, $\mathbf{R}_b^t$ and $\mathbf{R}_f^t$ will be derived later.

2.2.2. Fluid domain

The water in the reservoir is modeled as a linear[†] inviscid, irrotational and compressible fluid moving with zero mean velocity. The boundary conditions for the fluid domain are

$$\nabla p \cdot \mathbf{n}_h = -\rho \mathbf{n}_h \cdot \ddot{\mathbf{r}}_h^t, \qquad \text{at } \Gamma_h \text{, the upstream face of the dam} \tag{2a}$$

$$\nabla p \cdot \mathbf{n}_b + q\dot{p} = -\rho \mathbf{n}_b \cdot \ddot{\mathbf{r}}_b^t, \qquad \text{at } \Gamma_b \text{, the reservoir bottom} \tag{2b}$$

$$p = 0, \qquad \text{at the free water surface} \tag{2c}$$

where p is the hydrodynamic pressure in the water (in excess of hydrostatic pressure), $\mathbf{n}_h$ and $\mathbf{n}_b$ are the outward normal vectors to the fluid boundaries Γ_h and Γ_b, respectively; and ρ is the density of water. In addition to the boundary conditions of Eq. (2), an appropriate radiation condition must hold at the absorbing boundary Γ_r. The second term on the left side of Eq. (2b) represents the partial absorption of incident hydrodynamic pressure waves by sediments invariably deposited at the reservoir bottom, where the damping coefficient q is given by

$$qC = \frac{1-\alpha}{1+\alpha} \tag{3}$$

where C is the speed of pressure waves in water and α is the reservoir bottom reflection coefficient [12,29]. More sophisticated models for the reservoir bottom materials, such as a viscoelastic [30] or poroelastic layer [31] are also available.

Discretizing the fluid domain as a finite-element system and defining $\mathbf{p}^t$ as the vector of hydrodynamic pressures – where the superscript t has been added for consistency with the notation for the total displacements $\mathbf{r}^t$ – the standard discretization process results in

$$\mathbf{s}\ddot{\mathbf{p}}^t + \mathbf{b}\dot{\mathbf{p}}^t + \mathbf{h}\mathbf{p}^t = -\rho\left[\mathbf{Q}_h^{\mathrm{T}} + \mathbf{Q}_b^{\mathrm{T}}\right]\ddot{\mathbf{r}}^t + \mathbf{H}_r^t \tag{4}$$

where $\mathbf{s}$, $\mathbf{b}$ and $\mathbf{h}$ are the "mass", "damping" and "stiffness" matrices of the fluid [32], and $\mathbf{H}_r^t$ is the vector of forces associated with the absorbing boundary Γ_r due to the radiation condition and the contribution from earthquake-induced pressures in the part of the fluid that has been eliminated. An expression for these forces will be derived later.

The matrix $\mathbf{Q}_h$ relates hydrodynamic pressures in the fluid to accelerations of the dam at the dam-water interface Γ_h according to the boundary condition of Eq. (2a):

$$\mathbf{Q}_h = \int_{\Gamma_h} \bar{\mathbf{N}}_h^{\mathrm{T}} \mathbf{n}_h \mathbf{N}_h d\Gamma \tag{5}$$

where $\bar{\mathbf{N}}_h$ and $\mathbf{N}_h$ are the matrices of shape functions associated with the dam nodes and fluid nodes, respectively, on the interface Γ_h. The matrix $\mathbf{Q}_b$ is computed similarly, but integrated over the interface Γ_b.

[†] The subsequent formulation assumes, solely for convenience of notation, linear behavior also in the irregular part of the fluid domain.

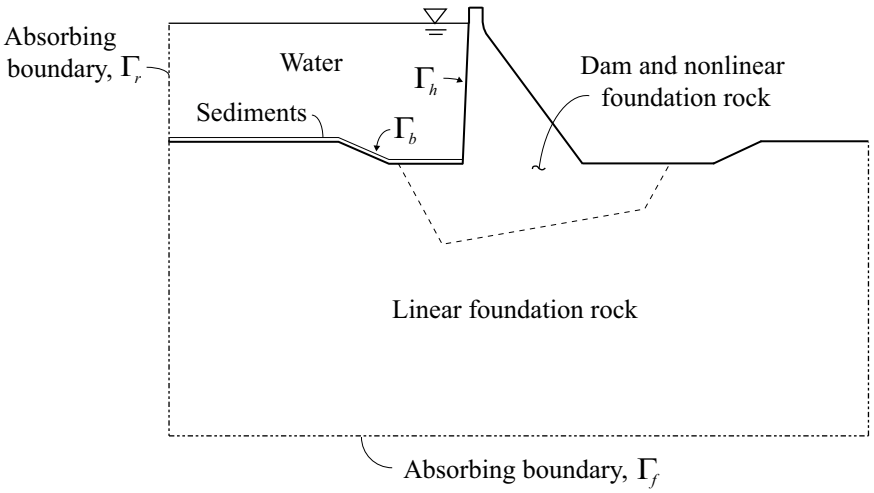

Figure 3. Schematic overview of finite-element model of the dam-water-foundation-rock system with semi-unbounded domains truncated by absorbing boundaries Γ_f and Γ_r.

3. INTERACTION AS A SCATTERING PROBLEM

Dam-water-foundation rock interaction may be viewed as a scattering problem in which the dam perturbs the "free-field" motion in an auxiliary state of the system. Procedures based on this idea have been developed for analysis of soil-structure interaction problems [22–24], and of dam-water-foundation rock systems using PML absorbing boundaries [25]. In this section, we will utilize these ideas to formulate an analysis procedure for the dam-water-foundation rock system with absorbing boundaries modeled by viscous dampers.

Consider the auxiliary water-foundation rock system defined in Fig. 4a. It consists of three subdomains: Ω^a denotes the foundation-rock region interior to the future absorbing boundary Γ_f; Ω_f^+ is the semi-unbounded foundation-rock region exterior to Γ_f; and Ω_r^+ is the prismatic fluid channel upstream of the future absorbing boundary Γ_r. This auxiliary system does not correspond to any physical state, but is introduced to facilitate formulation of the analysis procedure. The displacements and hydrodynamic pressures in the auxiliary water-foundation rock system are defined as $\mathbf{r}^a$ and $\mathbf{p}^a$, respectively.

The dam-water-foundation rock system is also separated into three subdomains (Fig. 4b): Ω denotes the dam and adjacent foundation rock and fluid regions interior to Γ_f and Γ_r, and Ω_f^+ and Ω_r^+ are the semi-unbounded foundation-rock and fluid domains exterior to Γ_f and Γ_r; these are identical to the exterior regions of the auxiliary system. In order to subsequently formulate the governing equations for the absorbing boundaries in terms of free-field quantities, we define the displacement field and hydrodynamic pressure field in the dam-water-foundation rock system by the variables

$$\mathbf{r}^t \text{ and } \mathbf{p}^t, \qquad \text{in the interior region } \Omega \tag{6a}$$

$$\mathbf{r}^t - \mathbf{r}^a \text{ and } \mathbf{p}^t - \mathbf{p}^a, \qquad \text{in the exterior regions } \Omega_f^+ \text{ and } \Omega_r^+ \tag{6b}$$

The variables chosen in Ω_f^+ and Ω_r^+ represent the *scattered motion* and *scattered hydrodynamic pressures*, i.e., the perturbation of the motion and pressures in the auxiliary water-foundation rock system due to the presence of the dam and irregular foundation-rock and fluid regions. This choice of variables in the exterior domains will subsequently allow us to formulate the governing equations for the absorbing boundaries in a way that the unknown forces $\mathbf{R}_f^t$ and $\mathbf{H}_r^t$ associated with Γ_f and Γ_r (Eqs. 1 and 4) can be determined from $\mathbf{r}^a$ and $\mathbf{p}^a$.

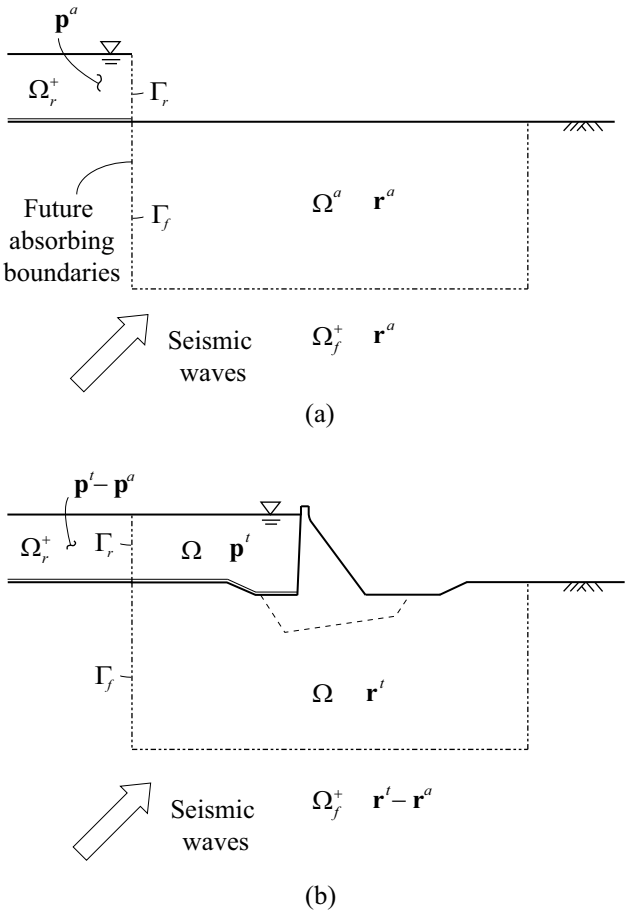

Figure 4. Illustration of dam-water-foundation rock interaction as a scattering problem: (a) auxiliary water-foundation rock system in its "free-field" state with variables defined by $\mathbf{p}^a$ in Ω_r^+ and $\mathbf{r}^a$ in $\Omega^a \cup \Omega_f^+$; (b) dam-water-foundation rock system with variables defined by $\mathbf{p}^t$ and $\mathbf{r}^t$ in Ω and the scattered variables $\mathbf{p}^t - \mathbf{p}^a$ in Ω_r^+ and $\mathbf{r}^t - \mathbf{r}^a$ in Ω_f^+.

4. VISCOUS DAMPER ABSORBING BOUNDARIES

A set of continuously distributed viscous dampers enforces the one-dimensional radiation condition for waves that impinge perpendicular to the foundation-rock boundaries [28]:

$$\sigma + \rho_f V_p \dot{u} = 0 \qquad \tau + \rho_f V_s \dot{w} = 0 \tag{7}$$

where σ and τ are the normal and tangential boundary tractions; u and w are the normal and

tangential displacements[†]; ρ_f is the density of the foundation medium; and V_p and V_s its pressure-wave velocity and shear-wave velocity. The viscous damper is a perfect absorber of body waves that arrive normal to the boundary, but only a partial absorber for body waves impinging at an arbitrary angle and for surface waves. However, the accuracy is generally acceptable provided the boundary is placed at sufficient distance from the wave source [17].

The viscous-damper boundary models the semi-unbounded foundation-rock region Ω_f^+ where the displacements were defined by the scattered motion (Eq. 6b), i.e., $u = u^t - u^a$ and $w = w^t - w^a$. Because the foundation rock in Ω_f^+ is assumed to be linear, it follows that the tractions associated with the scattered motion are $\sigma = \sigma^t - \sigma^a$ and $\tau = \tau^t - \tau^a$, where σ^a and τ^a are the tractions of the auxiliary water-foundation rock system. Substituting for the scattered motion and the corresponding boundary tractions in Eq. (7) and rearranging terms we obtain

$$\sigma^t = \sigma^a - \rho_f V_p \left(\dot{u}^t - \dot{u}^a \right) \qquad \tau^t = \tau^a - \rho_f V_s \left(\dot{w}^t - \dot{w}^a \right) \tag{8}$$

At the upstream truncation of the reservoir , the distributed viscous dampers enforce the one-dimensional radiation condition for a fluid [32]:

$$\frac{\partial p}{\partial n} + \frac{1}{C} \dot{p} = 0 \tag{9}$$

where n denotes the outward normal to the fluid boundary. This viscous-damper boundary models the unbounded prismatic fluid channel Ω_r^+ where the scattered pressures $p^t - p^a$ was chosen as the primary variable (Eq. 6b). Substituting for these in Eq. (9) and rearranging terms we obtain

$$\frac{\partial p^t}{\partial n} = \frac{\partial p^a}{\partial n} - \frac{1}{C} \left(\dot{p}^t - \dot{p}^a \right) \tag{10}$$

The distributed dampers described by Eqs. (7) to (10) can be lumped at the boundary nodes in a discretized model, resulting in discrete viscous dampers with coefficients

$$c_p = A \rho_f V_p \qquad c_s = A \rho_f V_s \qquad c_r = A / C \tag{11}$$

where c_p, c_s and c_r are the coefficients normal and tangential to the foundation-rock boundary, and at the fluid boundary, respectively, and A is the tributary area (tributary length in a 2D model) for the boundary node.

5. EQUATIONS OF MOTION

The hydrodynamic forces $\mathbf{R}_h^t$ and $\mathbf{R}_b^t$ in Eq. (1) that act on the dam and foundation rock, respectively, can be expressed in terms of the hydrodynamic pressures $\mathbf{p}^t$ as [32]

$$\mathbf{R}_h^t = \mathbf{Q}_h \, \mathbf{p}_h^t \qquad \mathbf{R}_b^t = \mathbf{Q}_b \, \mathbf{p}_b^t \tag{12}$$

[†] Temporarily – for convenience of notation – we use u and w instead of $\mathbf{r}^t$ for displacements.

Substituting these expressions into Eq. (1) and combining with Eq. (4) gives the equations of motion for the dam-water-foundation rock system with absorbing boundaries:

$$\begin{bmatrix} \mathbf{m} & \mathbf{0} \\ \rho(\mathbf{Q}_h^{\mathrm{T}} + \mathbf{Q}_b^{\mathrm{T}}) & \mathbf{s} \end{bmatrix} \begin{Bmatrix} \ddot{\mathbf{r}}^t \\ \ddot{\mathbf{p}}^t \end{Bmatrix} + \begin{bmatrix} \mathbf{c} & \mathbf{0} \\ \mathbf{0} & \mathbf{b} \end{bmatrix} \begin{Bmatrix} \dot{\mathbf{r}}^t \\ \dot{\mathbf{p}}^t \end{Bmatrix} + \begin{Bmatrix} \mathbf{f}(\mathbf{r}^t) \\ \mathbf{0} \end{Bmatrix} + \begin{bmatrix} \mathbf{0} & -(\mathbf{Q}_h + \mathbf{Q}_b) \\ \mathbf{0} & \mathbf{h} \end{bmatrix} \begin{Bmatrix} \mathbf{r}^t \\ \mathbf{p}^t \end{Bmatrix} = \begin{Bmatrix} \mathbf{R}_f^t + \mathbf{R}^{\mathrm{st}} \\ \mathbf{H}_r^t \end{Bmatrix} \tag{13}$$

where the coupling matrices $\mathbf{Q}_h$ and $\mathbf{Q}_b$ have non-zero entries only on the interfaces Γ_h and Γ_b, respectively. The forces $\mathbf{R}_f^t$ and $\mathbf{H}_r^t$ associated with the absorbing boundaries Γ_f and Γ_r are defined by the boundary conditions of Eqs. (8) and (10). These can be written in finite-element notation as

$$\mathbf{R}_f^t = \mathbf{R}_f^a - \mathbf{c}_f \left[\dot{\mathbf{r}}_f^t - \dot{\mathbf{r}}_f^a \right] \qquad \mathbf{H}_r^t = \mathbf{H}_r^a - \mathbf{c}_r \left[\dot{\mathbf{p}}_r^t - \dot{\mathbf{p}}_r^a \right] \tag{14}$$

where $\mathbf{c}_f$ is the matrix of damper coefficients c_p and c_s; $\mathbf{c}_r$ is the matrix of damping coefficients c_r; $\mathbf{R}_f^a$ are the forces consistent with the boundary tractions σ^a and τ^a at Γ_f; and $\mathbf{H}_r^a$ the forces consistent with the hydrodynamic pressure gradient $\partial p^a / \partial n$ at Γ_r. The vectors $\mathbf{R}_f^t$, $\mathbf{R}_f^a$, and matrix $\mathbf{c}_f$ contain non-zero entries only for nodes on Γ_f; and $\mathbf{H}_r^t$, $\mathbf{H}_r^a$, and $\mathbf{c}_r$ contain non-zero entries only for nodes on Γ_r.

Included in Eq. (13) are various interaction effects: dam-foundation rock interaction is included directly in the finite-element system matrices, dam-water and water-foundation rock interaction is represented by the coupling matrices $\mathbf{Q}_h$ and $\mathbf{Q}_b$, respectively, and reservoir bottom absorption is represented through the damping matrix $\mathbf{b}$.

Water-foundation rock interaction is also considered in the exterior domain $\Omega_f^+ \cup \Omega_r^+$ through the variables in Eq. (14): the displacements $\mathbf{r}_f^a$ and forces $\mathbf{R}_f^a$ at Γ_f include the effects of hydrodynamic pressures on the foundation-rock motion, and the pressures $\mathbf{p}_r^a$ and forces $\mathbf{H}_r^a$ at Γ_r include the effects of foundation-rock flexibility on the hydrodynamic pressures.

5.1. Approximating water-foundation rock interaction

These quantities are to be determined by analysis of the auxiliary water-foundation rock system (Fig. 4a). This expensive analysis may be simplified by ignoring the effects of water-foundation rock interaction in $\Omega_f^+ \cup \Omega_r^+$ by introducing the following approximations:

$$\mathbf{r}_f^a \approx \mathbf{r}_f^0 \text{ and } \mathbf{R}_f^a \approx \mathbf{R}_f^0 \text{ in the foundation-rock domain } \Omega^a \cup \Omega_f^+ \tag{15a}$$

$$\mathbf{p}_r^a \approx \mathbf{p}_r^0 \text{ and } \mathbf{H}_r^a \approx \mathbf{H}_r^0 \equiv \mathbf{0}^{\dagger} \text{ in the fluid domain } \Omega_r^+ \tag{15b}$$

where the *free-field motion* $\mathbf{r}_f^0$ and forces $\mathbf{R}_f^0$ at the boundary Γ_f are computed from analysis of $\Omega^a \cup \Omega_f^+$ – the foundation-rock part of Fig. 4a – alone, thus ignoring the effects of hydrodynamic pressures in Ω_r^+ on the foundation-rock motions; and the *free-field hydrodynamic*

---

† The forces $\mathbf{H}_r^0$ are zero for both horizontal and vertical ground motion because the pressure gradient $\partial p^0 / \partial n$ at Γ_r is zero when the foundation rock is rigid and the reservoir bottom is horizontal.

pressures $\mathbf{p}_r^0$ and forces $\mathbf{H}_r^0$ are computed from analysis of Ω_r^+ – the fluid part of Fig. 4a – alone with rigid foundation rock, thus ignoring the effects of foundation-rock flexibility on the hydrodynamic pressures in Ω_r^+. It has been demonstrated through numerical results that the response of gravity dams to horizontal ground motion is essentially unaffected by this approximation of water-foundation rock interaction, and that the response to vertical ground motion is affected noticeably only for large values of the wave-reflection coefficient α, where the approximate result tends to overestimate the response near resonant peaks [25].

Although the secondary effects of water-foundation rock interaction in $\Omega_f^+ \cup \Omega_r^+$ are neglected, the dominant effects within the truncated finite-element domain Ω are still rigorously represented by the coupling matrix $\mathbf{Q}_b$.

5.2. Final equations of motion

With the preceding approximations in modeling water-foundation rock interaction, the forces $\mathbf{R}_f^t$ and $\mathbf{H}_r^t$ can be determined independently of each other by consideration of the individual parts of the auxiliary system, $\Omega^a \cup \Omega_f^+$ and Ω_r^+, respectively. Substituting Eq. (14) with the approximations in Eq. (15) into Eq. (13), we obtain the final equations of motion for the dam-water-foundation rock system:

$$\begin{bmatrix} \mathbf{m} & \mathbf{0} \\ \rho(\mathbf{Q}_h^{\mathrm{T}} + \mathbf{Q}_b^{\mathrm{T}}) & \mathbf{s} \end{bmatrix} \begin{Bmatrix} \ddot{\mathbf{r}}^t \\ \ddot{\mathbf{p}}^t \end{Bmatrix} + \begin{bmatrix} \mathbf{c} + \mathbf{c}_f & \mathbf{0} \\ \mathbf{0} & \mathbf{b} + \mathbf{c}_r \end{bmatrix} \begin{Bmatrix} \dot{\mathbf{r}}^t \\ \dot{\mathbf{p}}^t \end{Bmatrix} + \begin{Bmatrix} \mathbf{f}(\mathbf{r}^t) \\ \mathbf{0} \end{Bmatrix} + \begin{bmatrix} \mathbf{0} & -(\mathbf{Q}_h + \mathbf{Q}_b) \\ \mathbf{0} & \mathbf{h} \end{bmatrix} \begin{Bmatrix} \mathbf{r}^t \\ \mathbf{p}^t \end{Bmatrix} = \begin{Bmatrix} \mathbf{R}^{\mathrm{st}} \\ \mathbf{0} \end{Bmatrix} + \begin{Bmatrix} \mathbf{P}_f^0 \\ \mathbf{P}_r^0 \end{Bmatrix} \tag{16}$$

where the *effective earthquake forces* are

$$\mathbf{P}_f^0 = \mathbf{R}_f^0 + \mathbf{c}_f \dot{\mathbf{r}}_f^0 \text{ at the foundation-rock boundary } \Gamma_f \tag{17a}$$

$$\mathbf{P}_r^0 = \mathbf{c}_r \dot{\mathbf{p}}_r^0 \text{ at the fluid boundary } \Gamma_r \tag{17b}$$

Observe by comparing Eqs. (16) and (13) that the unknown forces $\mathbf{R}_f^t$ associated with the absorbing boundary Γ_f have now been expressed in terms of the viscous damper forces $\mathbf{c}_f \dot{\mathbf{r}}^t$ and the effective earthquake forces $\mathbf{P}_f^0$, and $\mathbf{H}_r^t$ associated with Γ_r have been expressed in terms of the viscous damper forces $\mathbf{c}_r \dot{\mathbf{p}}^t$ and the effective earthquake forces $\mathbf{P}_r^0$. Working with the scattered variables in Ω_f^+ and Ω_r^+, and approximating water-foundation rock interaction, has enabled us to derive Eq. (17) for the effective earthquake forces in terms of free-field variables only.

In the finite-element model, interface elements are introduced at the dam-water interface Γ_h and water-foundation rock interface Γ_b to couple the dam and foundation-rock with the fluid domain through Eq. (5) localized to the element level. Assembly of the interface element matrices produces the global matrices involving $\mathbf{Q}_h$ and $\mathbf{Q}_b$ in Eq. (16). These coupling terms lead to an unsymmetric system of global equations, but this does not pose any major complications because recent advances in computer power and equation-solver technology have greatly reduced the computational time required to solve sparse unsymmetric systems of linear equations.

6. FREE-FIELD EARTHQUAKE MOTION

The free-field motion $\mathbf{r}_f^0$ required to compute the effective earthquake forces $\mathbf{P}_f^0$ can be determined by various methods. The most general approach is to perform a large-scale simulation of seismic wave propagation from an earthquake source to the dam site using physics-based 3D finite-element or finite-difference models of large regions [33]. The ability of such models to generate accurate results depends on the quality of the information available regarding the earthquake faults and their rupture characteristics, the geological materials between the earthquake source and the site, and local site conditions. Because this information is rarely available, such simulations are impractical at the present time, especially for defining motions in the high frequency range that is relevant for concrete dams.

Therefore, the standard procedure is to define the ground motion at the control point (Fig. 1) to be consistent with a design spectrum. This target spectrum may be the uniform hazard spectrum (UHS) determined by probabilistic seismic hazard analysis (PSHA), or a conditional mean spectrum. Recorded ground motions are selected, scaled and modified to "match" in some sense the target spectrum; alternatively synthetic motions may be developed for an earthquake scenario. These methods are well developed for a single component of ground motion; work on extending these methods to two- or three components is in progress.

To determine the required free-field motion $\mathbf{r}_f^0$ at the boundary Γ_f from the ground motion at the control point it is necessary to introduce assumptions on the type of seismic waves and their incidence angle. The simplest assumption, often used for site response analyses and soil-structure interaction analyses, is vertically propagating SH-waves and P-waves [16,34]. This is clearly a major simplification of the actual seismic wave field, which generally consists of a combination of vertically and horizontally propagating SH-, SV- and P-waves, and horizontally propagating surface waves, but at the present time it seems to be the only pragmatic choice.

Under the assumption of vertically propagating body waves and homogeneous or layered rock in $\Omega^a \cup \Omega_f^+$, the free-field motion $\mathbf{r}_f^0$ at Γ_f can be obtained by one-dimensional deconvolution of the ground motion at the control point, $a_g^k(t)$, using well-known procedures; software such as SHAKE [34] or DeepSoil [35] can be utilized for this purpose. In principle, the deconvolution analysis can provide directly the motion at every nodal point on Γ_f, but this approach may become cumbersome for a large number of elevations. An alternative method that overcomes this problem is presented in the next section.

7. COMPUTING EFFECTIVE EARTHQUAKE FORCES

7.1. Effective earthquake forces at foundation-rock boundary

7.1.1. Bottom boundary

Following the method first proposed by Joyner and Chen [36], where the boundary tractions are reformulated in terms of the incident and reflected seismic waves, the effective earthquake forces at the bottom boundary can be expressed as:

$$\mathbf{P}_f^0 = 2\mathbf{c}_f\,\dot{\mathbf{r}}_I^0 \tag{18}$$

where $\mathbf{r}_I^0$ is the motion at the bottom boundary due to the incident (upward propagating) seismic waves. This equation has the distinct advantage in that it requires only the motion $\mathbf{r}_I^0$ of the incident wave, thus avoiding computation of the free-field tractions required in Eq. (17a). Furthermore, the incident motion $\mathbf{r}_I^0$ is easily computed as 1/2 the *outcrop motion*[†] at the bottom boundary, which is extracted directly from the deconvolution analysis.

7.1.2. Vertical side boundaries

The free-field motion $\mathbf{r}_f^0$ (and its time derivatives) required to compute the effective earthquake forces $\mathbf{P}_f^0$ at the vertical side boundaries can be obtained directly from the deconvolution analysis; free-field tractions are then computed from one-dimensional stress-strain relations and these stresses converted to forces. Alternatively, both quantities can be computed by an analysis of the foundation rock in its free-field state: $\Omega^a \cup \Omega_f^+$ in Fig. 4a. Analysis of this system reduces to a single column of foundation-rock elements with a viscous damper at its base that is subjected to the forces of Eq. (18) and analyzed to determine $\dot{\mathbf{r}}_f^0$ and $\mathbf{R}_f^0$ at each nodal point along the height (Fig. 5a).

Although straightforward, both of these approaches require the force histories $\mathbf{P}_f^0$ at all nodal points on the vertical boundaries to be stored for later use in setting up Eq. (17a). Clearly, such "book-keeping" may become cumbersome for large models, especially for a three-dimensional system [21]. These difficulties can be avoided by introducing free-field boundary elements in the form of one-dimensional foundation-rock columns at the vertical boundaries that are solved in parallel with the main FE model. Such elements have been implemented in ABAQUS [37] and FLAC [38]; a complete element formulation can be found in ref. [37].

7.2. Effective earthquake forces at fluid boundary

The effective earthquake forces $\mathbf{P}_r^0$ at Γ_r are to be computed by analysis of the prismatic fluid channel of uniform depth: Ω_r^+ in Fig. 4a with rigid foundation rock. Horizontal ground motion will not generate any hydrodynamic pressures because the reservoir bottom is horizontal, hence $\mathbf{P}_r^0 = \mathbf{0}$. Analysis of the prismatic channel to vertical ground motion reduces to a single column of fluid elements of unit width subjected to the force $-\rho\, a_g^y$ at its base (Fig. 5b). This analysis provides the pressures $\mathbf{p}_r^0$ (and its time derivatives) that enter in Eq. (17b).

8. SUMMARY OF PROCEDURE

Analysis of the dam-water-foundation rock system subjected to the free-field ground acceleration $a_g^k(t)$, $k = x, y$, defined at a control point on the surface of the foundation rock (Fig. 1) is organized in three major phases: initial static analysis, linear analyses of the free-field foundation-rock and fluid systems, and nonlinear dynamic analysis of the dam-water-foundation rock system.

[†] The reflected motion must equal the incident motion at every rock outcrop (stress-free boundary), hence is the incident motion identically equal to 1/2 the outcrop motion.

Initial static analysis:

1. Develop a finite-element model for static analysis of the dam-foundation rock system with an appropriate material model for the dam concrete and an appropriate (static) model for the semi-unbounded foundation rock.
2. Compute the static response of this system to hydrostatic forces and the self-weight of the dam and foundation rock.
3. Record the static state of the dam and foundation rock, including displacements, stresses and strains, and reactions from the foundation rock at the boundary Γ_f.

Linear analysis of the free-field foundation rock (Fig. 5a):

4. Obtain the free-field motion at the base of the foundation-rock model by deconvolution of the surface ground motion $a_g^k(t)$.
5. Calculate the effective earthquake forces $\mathbf{P}_f^0$ at the bottom boundary of the foundation-rock domain from Eq. (18), with the motion $\mathbf{r}_I^0$ due to the incident (upward propagating) seismic wave taken as 1/2 the outcrop motion extracted from the deconvolution analysis.
6. Develop a finite-element model for the free-field foundation rock: a single column of elements that has the same mesh density as the main FE model adjacent to the vertical boundaries, with viscous dampers at the base in the *x*- and *y*-directions.
7. Compute $\dot{\mathbf{r}}_f^0$ and $\mathbf{R}_f^0$ at each nodal point along the height by analyzing the foundation-rock column subjected to forces given by Eq. (18) at its base.
8. Calculate the effective earthquake forces $\mathbf{P}_f^0$ at the vertical boundaries of the foundation-rock domain from Eq. (17a) using $\dot{\mathbf{r}}_f^0$ and $\mathbf{R}_f^0$ from Step 7.

Steps 6-8 may be avoided if free-field boundary elements [37] are added along the vertical boundaries.

Linear analysis of the free-field fluid (Fig. 5b):

9. Develop a finite-element model for the free-field fluid: a single column of elements of unit width with the same vertical mesh density as the fluid adjacent to the boundary Γ_r, add a single line element to model reservoir bottom sediments.
10. Calculate $\dot{\mathbf{p}}_r^0$ at every nodal point along the height by analyzing the fluid column subjected to the force $-\rho a_g^y$ at its base.
11. Compute the effective earthquake forces $\mathbf{P}_r^0$ at the fluid boundary Γ_r from Eq. (17b) using $\dot{\mathbf{p}}_r^0$ from Step 10.

Analysis of the free-field fluid system (Steps 9-11) is not necessary if the ground motion is purely horizontal.

Nonlinear dynamic analysis of dam-water-foundation rock system (Fig. 5c):

12. Develop a finite-element model of the dam-water-foundation rock system with viscous damper boundaries to truncate the semi-unbounded foundation-rock and fluid domains at Γ_f and Γ_r, respectively, using solid and fluid elements for the dam, foundation rock, and fluid, as well as dam-water and water-foundation rock interface elements, and line elements for the reservoir bottom sediments.
13. Calculate the response of the finite-element model of the dam-water-foundation rock system subjected to the effective earthquake forces $\mathbf{P}_f^0$ at the boundary Γ_f computed in Steps 5 and 8, $\mathbf{P}_r^0$ at the boundary Γ_r calculated in Step 11, as well as self-weight, hydrostatic forces and static foundation-rock reactions at Γ_f. The static state of the dam (Step 3) is taken as the initial state in the nonlinear dynamic analysis. This phase of the analysis is implemented by solving Eq. (16).

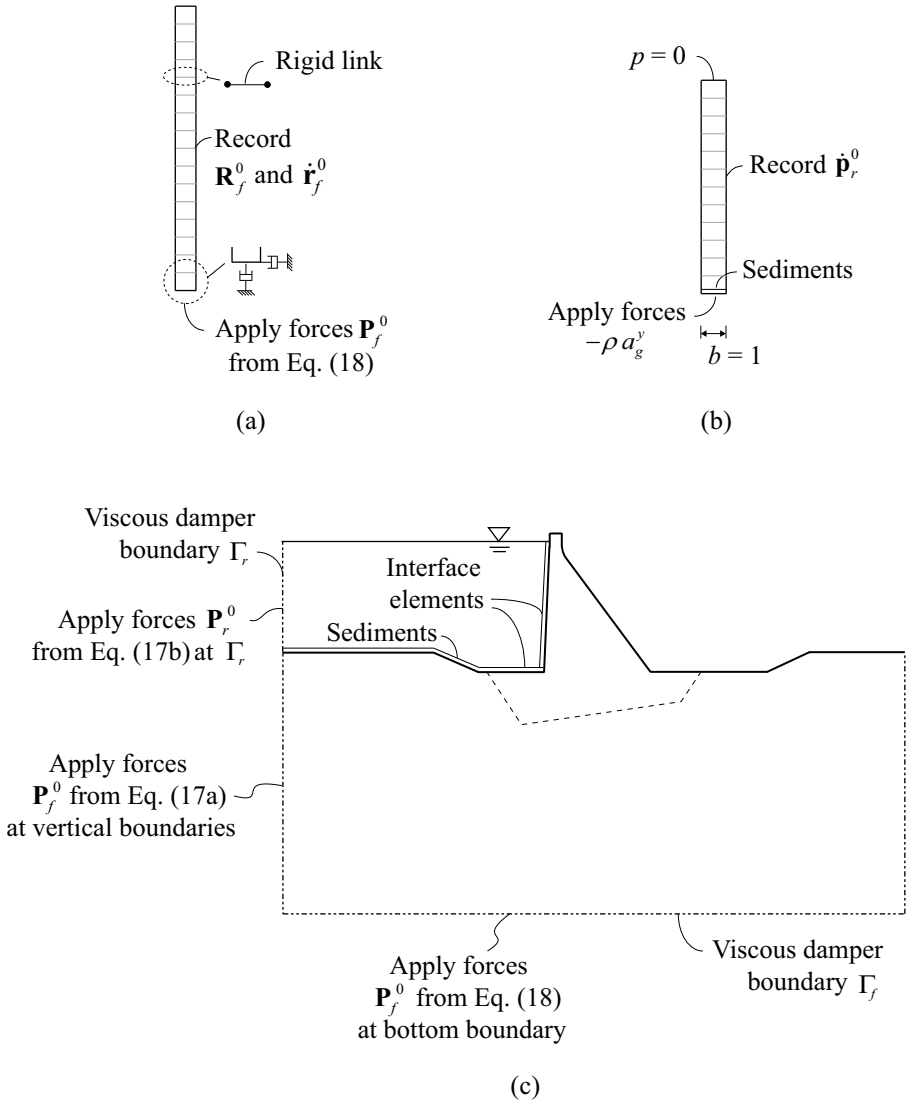

Figure 5. Summary of analysis procedure: (a) analysis of single column of foundation-rock elements to compute $\dot{\mathbf{r}}_f^0$ and $\mathbf{R}_f^0$; (b) analysis of single column of fluid elements to calculate $\dot{\mathbf{p}}_r^0$ for vertical ground motion; (c) application of effective earthquake forces to truncated FE model.

9. NUMERICAL VALIDATION

9.1. System analyzed

The analysis procedure developed in the preceding sections is implemented in OpenSees [39] and validated numerically by computing the dynamic response of the idealized dam-water-foundation rock system shown in Fig. 6. The idealized dam has a triangular cross-section of height H = 120 m, a vertical upstream face and a downstream face with a slope of 0.8 to 1. The concrete in the dam is assumed to be homogeneous, isotropic and linearly elastic, in a state of generalized plane stress, with modulus of elasticity E_s = 22.4 GPa, density ρ_s = 2483 kg/m^3, and Poisson's ratio ν_s = 0.20. The foundation rock is assumed to be homogeneous, isotropic and linearly elastic, in a state of generalized plane stress, with modulus of elasticity E_f = 22.4 GPa (i.e. E_f / E_s = 1) density ρ_f = 2643 kg/m^3, and Poisson's ratio ν_f = 0.33. Material damping is modeled by Rayleigh damping with $\zeta_s = 2\%$ and $\zeta_f = 2\%$ viscous damping specified for the dam and foundation-rock separately; the damping matrix for the complete system is constructed by assembling the individual Rayleigh damping matrices for the two subdomains [40]. The impounded water has the same depth as the height of the dam, density ρ = 1000 kg/m^3, and pressure-wave velocity C = 1440 m/s. The reservoir-bottom reflection coefficient is selected as α = 0.75.

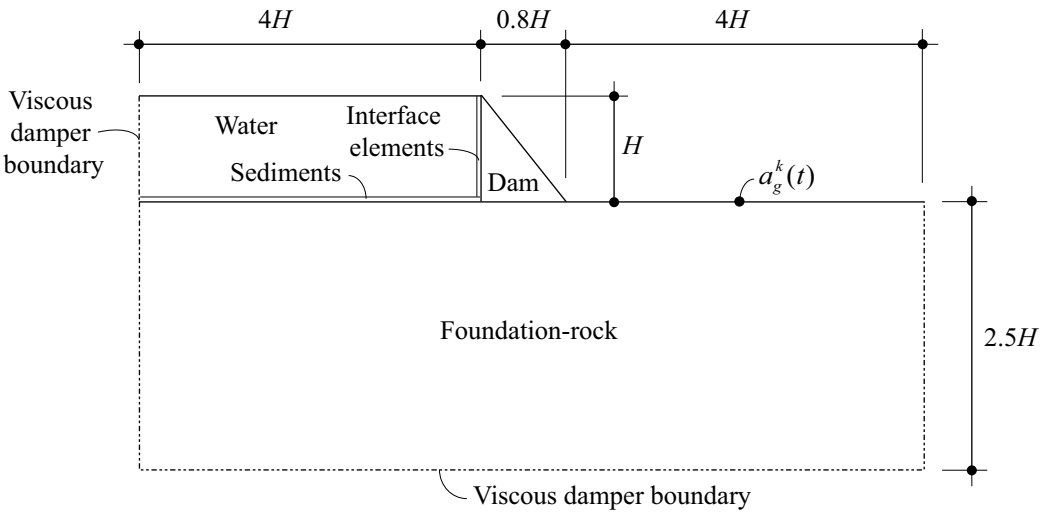

Figure 6. Schematic diagram of FE model for idealized dam-water-foundation rock system with viscous damper boundaries to truncate semi-unbounded foundation-rock and fluid domains.

The FE mesh for the dam has 15 elements along the base and 29 elements along the height. The FE meshes of the dam, foundation-rock and fluid domains match at their respective interfaces, with a gradually increasing element size towards the outer edges of the model. The maximum element size in the foundation-rock is limited to less than one-tenth of the shortest wavelength considered in the analysis to ensure satisfactory wave propagation in the mesh. The FE model includes solid and acoustic elements in the dam, foundation-rock and fluid domain; interface elements at the dam-water and water-foundation rock interfaces; and line elements at

the reservoir bottom. The width (on both sides of the dam) and depth of the foundation-rock domain is selected as 4*H* and 2.5*H*, respectively; these dimensions are considered sufficiently large to minimize wave reflections from the absorbing boundaries for the selected system parameters.

9.2. Frequency response functions for dam response

Frequency response functions are computed by time-domain analysis of the FE system with free-field surface motions $a_g^x(t)$ and $a_g^y(t)$ defined by a harmonic function of unit amplitude. The response of the dam for a single excitation frequency is computed by solving Eq. (16) for long enough time to determine the amplitude of the steady-state response. The response was also computed directly in the frequency domain by the substructure method [12] using the computer program EAGD84 [41]. In this program, the foundation rock is modeled as a viscoelastic halfspace, the fluid domain is treated as an infinitely long continuum, and the earthquake excitation is specified directly at the dam-foundation interface, thus avoiding the need for artificial model truncations, absorbing boundaries, and deconvolution of the ground motion.

Material damping in EAGD84 is modeled by constant hysteretic damping specified by the hysteretic damping factors $\eta_s = 0.04$ and $\eta_f = 0.04$ for the dam and foundation-rock; this corresponds to viscous damping ratios of $\zeta_s = 2\%$ and $\zeta_f = 2\%$. For time-domain analysisthe direct FE method, the Rayleigh coefficients a_0 and a_1 are determined by specifying ζ_s and ζ_f at the excitation frequency $f = \omega / 2\pi$, where ω is the angular frequency of the harmonic excitation, and at f = 1 Hz. This unconventional choice defines frequency-dependent Rayleigh damping to be as consistent as possible with frequency-independent hysteretic damping, thus ensuring a meaningful comparison of the frequency response functions from the direct FE and substructure methods. For the response history analyses to earthquake excitation presented in Section 9.3, the Rayleigh damping matrix is constructed by standard procedures [40].

9.2.1. Dam-foundation rock interaction

The frequency response functions for the amplitude of the relative horizontal acceleration at the crest of the dam on flexible foundation rock with empty reservoir are presented in Fig. 7. The results obtained by the direct method are generally close to those from the substructure method, thus validating its ability to model the semi-unbounded dam-foundation rock system. The discrepancies observable at some frequencies are due to the inability of the viscous damper boundary to perfectly absorb outgoing (scattered) waves from the dam; such discrepancies will generally decrease as the size of the foundation-rock domain included in the FE model increases.

The dam engineering profession has been using a variation of the rigorous method summarized in Section 8 wherein the effective earthquake forces $\mathbf{P}_f^0$ are applied only at the bottom boundary, i.e., the forces at the vertical side boundaries are neglected. Initiated by the US Bureau of Reclamation [15] and applied to actual projects [14,42], variations of the method have also been used by other dam engineering professionals [43].

The results obtained from such an analysis procedure are seen to be in significant error for both horizontal and vertical ground motion (Fig. 8). These discrepancies arise from the inability of this model to reproduce free-field conditions. Attempts have been made to correct for this shortcoming by modifying the amplitude and/or frequency content of the input ground

motion. However, it is not clear whether such modifications will lead to acceptable results, and neither version of the approximate method has been validated against the substructure method.

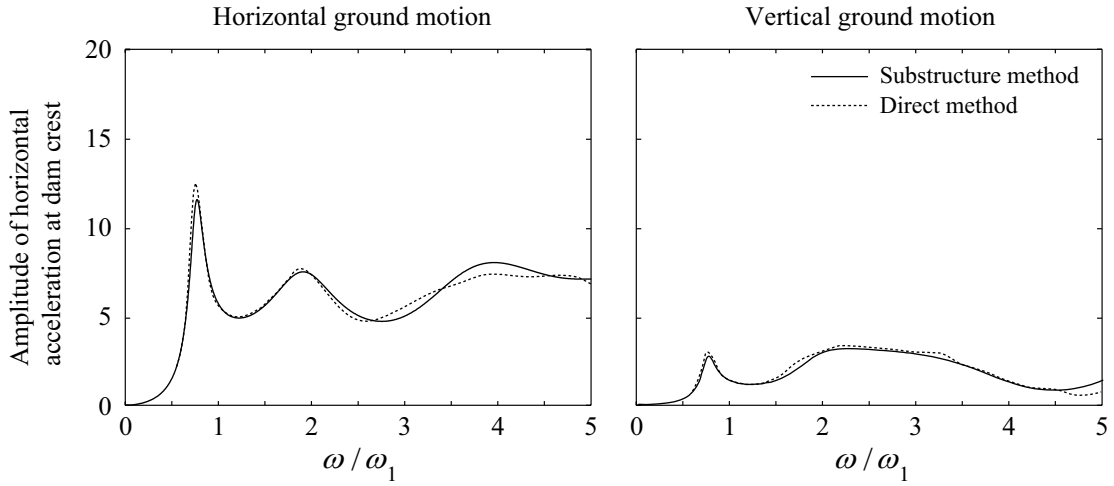

Figure 7. Comparison of frequency response functions from direct and substructure methods for the amplitude of relative horizontal acceleration at the crest of dam on flexible foundation rock due to horizontal and vertical ground motion. Results are plotted against normalized frequency ω/ω_1 where ω_1 is the fundamental frequency of the dam alone on rigid foundation.

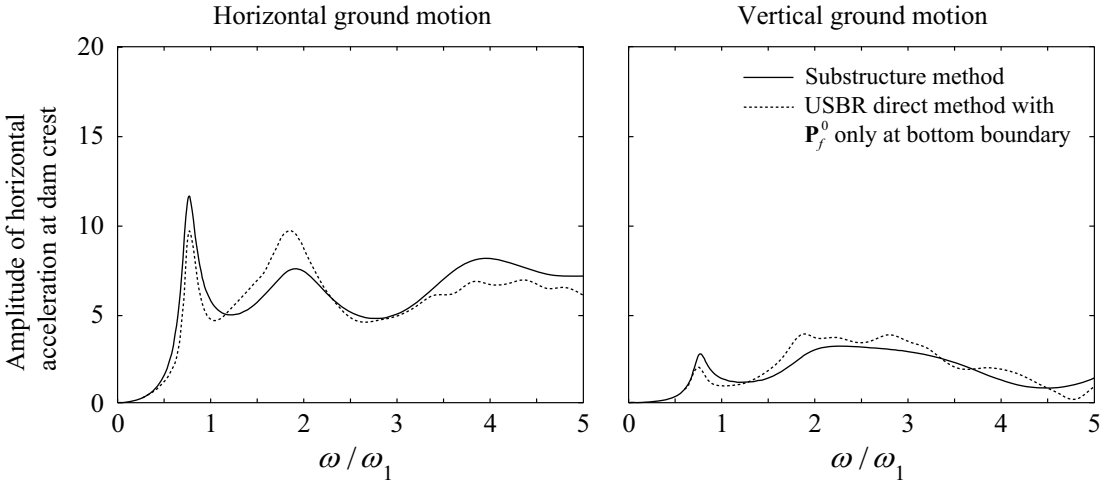

Figure 8. Comparison of frequency response functions from the USBR direct and substructure methods for the amplitude of relative horizontal acceleration at the crest of dam on flexible foundation rock due to horizontal and vertical ground motion. Results are plotted against normalized frequency ω/ω_1 where ω_1 is the fundamental frequency of the dam alone on rigid foundation.

9.2.2. Dam-water interaction

The frequency response functions for the amplitude of the relative horizontal acceleration at the crest of the dam on rigid foundation rock with impounded water are presented in Fig. 9, where the damping ratio for the dam alone is selected as $\zeta_s = 5\%$. The results from the direct method closely match the results of the substructure method for both horizontal and vertical ground motion, thus validating its ability to model the semi-unbounded fluid domain.

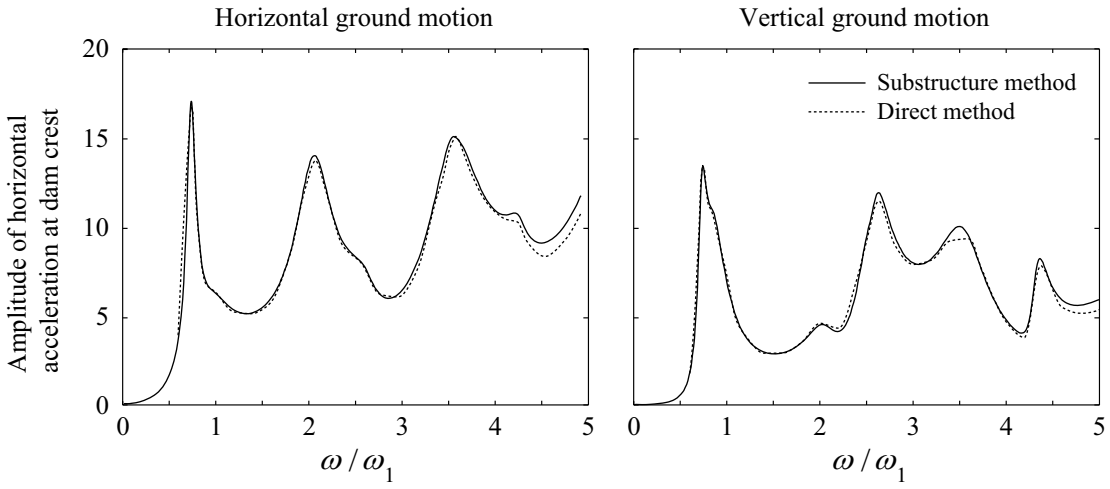

Figure 9. Comparison of frequency response functions from direct and substructure methods for the amplitude of relative horizontal acceleration at the crest of dam with impounded reservoir due to horizontal and vertical ground motion. Results are plotted against normalized frequency ω/ω_1 where ω_1 is the fundamental frequency of the dam alone on rigid foundation. $\zeta_s = 5\%$.

9.2.3. Dam-water-foundation rock interaction

The frequency response functions for the amplitude of the relative horizontal acceleration at the crest of the dam on flexible foundation rock with impounded water are shown in Fig. 10, where they are compared to the substructure method results. Because the computer program EAGD84 – where the substructure method is implemented – ignores water-foundation rock interaction completely, this interaction is also ignored in the direct method for these validation analyses.

The results computed by the direct method are generally close to the results from the substructure method for both vertical and horizontal ground motion, thus validating its ability to model the semi-unbounded dam-water-foundation rock system. The slight differences are attributable to the approximate nature of the viscous damper boundary, which is unable to perfectly absorb all outgoing waves.

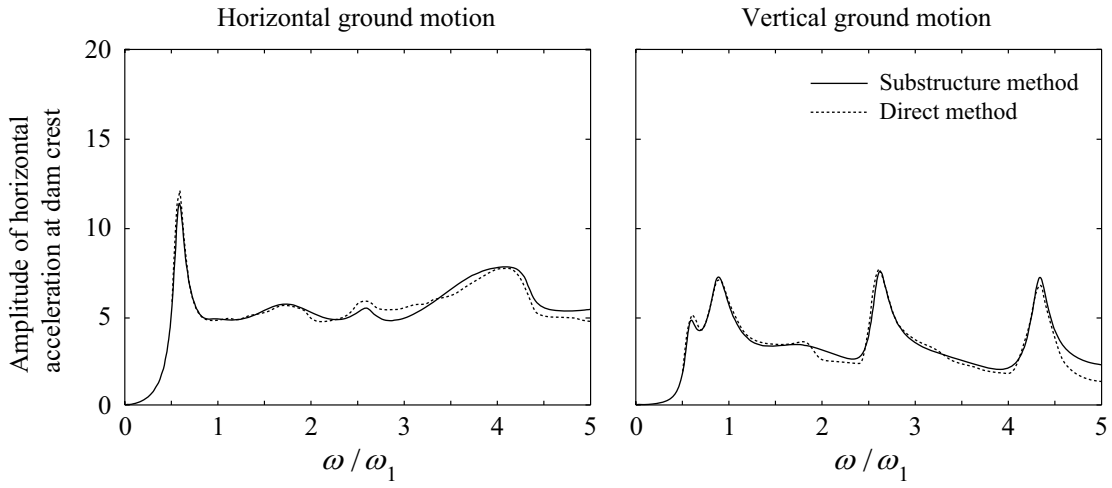

Figure 10. Comparison of frequency response functions from direct and substructure methods for the amplitude of relative horizontal acceleration at the crest of dam on flexible foundation rock with impounded reservoir due to horizontal and vertical ground motion. Results are plotted against normalized frequency ω/ω_1 where ω_1 is the fundamental frequency of the dam alone on rigid foundation.

9.3. Response to transient motion

To demonstrate the ability of the direct method to accurately compute the response of the dam-water-foundation rock system to earthquake excitation, the system in Fig. 6 is analyzed for $a_g^x(t)$ and $a_g^y(t)$ specified as the S69E and vertical components, respectively, of the ground motion recorded at Taft Lincoln School Tunnel during the 1952 Kern County earthquake. The response was also computed by the substructure method. The relative horizontal displacements and accelerations at the crest of the dam are presented in Fig. 11, and the envelope values of the maximum principal stresses in Fig. 12. It can be seen that the results from the direct method closely match the results from the substructure method, as expected because of the close agreement observed earlier for the frequency response functions.

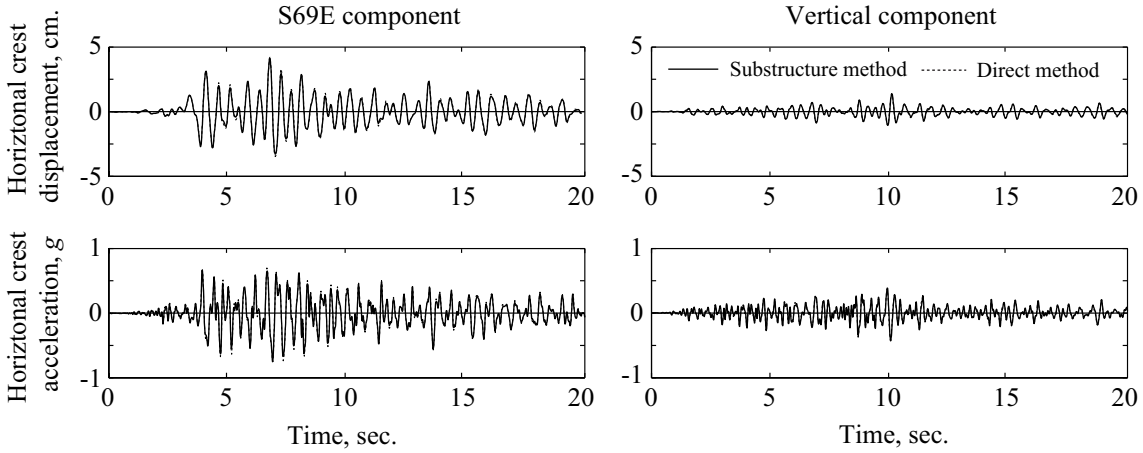

Figure 11. Relative horizontal displacements and accelerations at the crest of the dam on flexible foundation rock with impounded reservoir due to the S69E and vertical components, separately, of Taft ground motion. Results are computed by the direct and substructure methods.

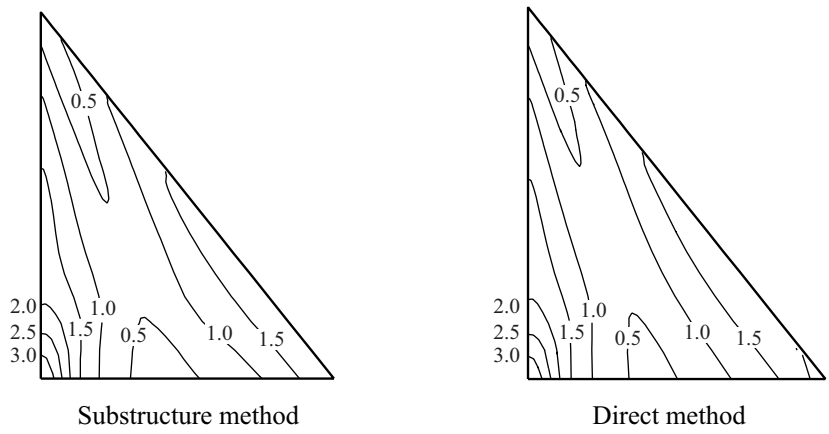

Figure 12. Envelope values of maximum principal stresses, in MPa, in dam on flexible foundation rock with impounded reservoir due to S69E component of Taft ground motion; initial static stresses are excluded. Results are computed by the direct and substructure methods.

10. CONCLUSIONS

We have developed a direct finite element method for earthquake analysis of concrete dams interacting with fluid and foundation rock, where the semi-unbounded fluid and foundation-rock domains are truncated by absorbing boundaries modeled by viscous dampers. The analysis procedure is formulated by interpreting dam-water-foundation rock interaction as a scattering problem [24,25] wherein the dam perturbs a free-field state of the system.

The use of finite elements permits (1) modeling of an arbitrarily shaped dam, foundation-rock surface and fluid domain, and (2) nonlinear modeling of the dam and adjacent parts of the foundation-rock and fluid domains. The FE model for the fluid includes water compressibility

and reservoir bottom sediments, and the FE model for the foundation-rock domain includes mass, stiffness, and material damping appropriate for rock. Thus, the unrealistic assumptions of massless rock and incompressible water, sometimes used in dam engineering practice, are eliminated.

The seismic input to the analysis procedure is the design ground motion specified at a control point on the free surface. The free-field motion at depth in the foundation-rock is determined by deconvolution of this motion. The effective earthquake forces at the boundaries of the foundation-rock and fluid domains are determined from analysis of two individual one-dimensional free-field systems. Implementation of these analyses is straightforward, and does not require modification of the source code of a commercial finite element program.

The analysis procedure has been validated numerically by computing the frequency response functions and transient response of an idealized dam-water-foundation rock system and comparing against results from the substructure method. The excellent agreement demonstrates that (1) the truncated foundation-rock and fluid models with viscous damper boundaries are able to model the semi-unbounded domains; (2) the earthquake excitation is properly defined by the effective earthquake forces determined from the free-field variables.

Because the analysis procedure is applicable to nonlinear systems, it allows for modeling of concrete cracking, as well as sliding and separation at construction joints, lift joints, and at concrete-rock interfaces. Implementation of the procedure is facilitated by commercial finite element software, with their nonlinear material models, that permit modeling of viscous damper boundaries and specification of effective earthquake forces at these boundaries.

ACKNOWLEDGEMENTS

The authors are grateful to Dr. Ushnish Basu for his advice and contributions to the development of the analysis procedure and its numerical implementation, and to Dr. Frank McKenna for his help implementing acoustic fluid elements for two-dimensional analysis in OpenSees. The first author would also like to thank Prof. Svein Remseth and Amir Kaynia at the Norwegian Univ. of Science and Technology (NTNU) for their encouragement and support.

REFERENCES

1. Chopra AK. Earthquake analysis of arch dams: Factors to be considered. *Journal of Structural Engineering* 2012; **138**(2): 205–214. DOI: 10.1061/(ASCE)ST.1943-541X.0000431.
2. Hall JF, Chopra AK. Hydrodynamic effects in the dynamic response of concrete gravity dams. *Earthquake Engineering & Structural Dynamics* 1982; **10**(2): 333–345. DOI: 10.1002/eqe.4290100212.
3. Fenves G, Chopra AK. Effects of reservoir bottom absorption and dam-water-foundation rock interaction on frequency response functions for concrete gravity dams. *Earthquake Engineering & Structural Dynamics* 1985; **13**(1): 13–31. DOI: 10.1002/eqe.4290130104.
4. Tan H, Chopra AK. Dam-foundation rock interaction effects in earthquake response of arch dams. *Journal of Structural Engineering* 1996; **122**(5): 528–538. DOI: 10.1061/(ASCE)0733-9445(1996)122:5(528).
5. Zhang C, Pan J, Wang JT. Influence of seismic input mechanisms and radiation damping on arch dam response. *Soil Dynamics and Earthquake Engineering* 2009; **29**(9): 1282–1293. DOI: 10.1016/j.soildyn.2009.03.003.
6. Chopra AK, Wang JT. Earthquake response of arch dams to spatially varying ground motion. *Earthquake Engineering & Structural Dynamics* 2009; **39**(8): 887–906. DOI: 10.1002/eqe.974.
7. Bhattacharjee SS, Léger P. Seismic cracking and energy dissipation in concrete gravity dams. *Earthquake*

Engineering & Structural Dynamics 1993; **22**(11): 991–1007. DOI: 10.1002/eqe.4290221106.
8. Cervera M, Oliver J, Faria R. Seismic evaluation of concrete dams via continuum damage models. *Earthquake Engineering & Structural Dynamics* 1995; **24**(9): 1225–1245. DOI: 10.1002/eqe.4290240905.
9. Fenves GL, Mojtahedi S, Reimer RB. Effect of contraction joints on earthquake response of an arch dam. *Journal of Structural Engineering* 1992; **118**(4): 1039–1055. DOI: 10.1061/(ASCE)0733-9445(1992)118:4(1039).
10. El-Aidi B, Hall JF. Non-linear earthquake response of concrete gravity dams part 1: Modelling. *Earthquake Engineering & Structural Dynamics* 1989; **18**(6): 837–851. DOI: 10.1002/eqe.4290180607.
11. Pan J, Zhang C, Xu Y, Jin F. A comparative study of the different procedures for seismic cracking analysis of concrete dams. *Soil Dynamics and Earthquake Engineering* 2011; **31**(11): 1594–1606. DOI: 10.1016/j.soildyn.2011.06.011.
12. Fenves G, Chopra AK. Earthquake analysis of concrete gravity dams including reservoir bottom absorption and dam-water-foundation rock interaction. *Earthquake Engineering & Structural Dynamics* 1984; **12**(5): 663–680. DOI: 10.1002/eqe.4290120507.
13. Tan H, Chopra AK. Earthquake analysis of arch dams including dam-water-foundation rock interaction. *Earthquake Engineering & Structural Dynamics* 1995; **24**(11): 1453–1474. DOI: 10.1002/eqe.4290241104.
14. Noble CR, Nuss L. Implicit and explicit nonlinear dynamic analysis of a large thin-arch dam using massively parallel computing. *Proc. for 13th World Conference on Earthquake Engineering*, Vancouver, Canada: 2004.
15. US Bureau of Reclamation. *State-of-Practice for the Nonlinear Analysis of Concrete Dams at the Bureau of Reclamation*. Denver, CO: 2006.
16. Wolf JP. *Dynamic Soil-structure Interaction*. Englewood Cliffs, NJ: Prentice Hall; 1985.
17. Wolf JP. *Soil-structure Interaction in Time Domain*. Englewood Cliffs, NJ: Prentice Hall; 1988.
18. Kellezi L. Local transmitting boundaries for transient elastic analysis. *Soil Dynamics and Earthquake Engineering* 2000; **19**(7): 533–547. DOI: 10.1016/S0267-7261(00)00029-4.
19. Zienkiewicz OC, Bicanic N, Shen FQ. Earthquake input definition and the transmitting boundary conditions. *Advances in Computational Nonlinear Mechanics*, Springer; 1989.
20. Lemos J V. Discrete element analysis of dam foundations. In: Sharma VM, Saxena KR, Woods RD, editors. *Distinct Element Modelling in Geomechanics*, Rotterdam: Balkema; 1999.
21. Saouma V, Miura F, Lebon G, Yagome Y. A simplified 3D model for soil-structure interaction with radiation damping and free field input. *Bulletin of Earthquake Engineering* 2011; **9**(5): 1387–1402. DOI: 10.1007/s10518-011-9261-7.
22. Bielak J, Christiano P. On the effective seismic input for non-linear soil-structure interaction systems. *Earthquake Engineering & Structural Dynamics* 1984; **12**(3): 107–119. DOI: 10.1002/eqe.4290120108.
23. Aydinoglu MN. Consistent formulation of direct and substructure methods in nonlinear soil-structure interaction. *Soil Dynamics and Earthquake Engineering* 1993; **12**(7): 403–410. DOI: 10.1016/0267-7261(93)90003-A.
24. Bielak J, Loukakis K, Hisada Y, Yoshimura C. Domain reduction method for three-dimensional earthquake modeling in localized regions, Part I: Theory. *Bulletin of the Seismological Society of America* 2003; **93**(2): 817–824. DOI: 10.1785/0120010251.
25. Basu U. Perfectly matched layers for acoustic and elastic waves: Theory, finite-element implementation and application to earthquake analysis of dam-water-foundation rock systems. PhD thesis, University of California, Berkeley, 2004.
26. Basu U, Chopra AK. Perfectly matched layers for transient elastodynamics of unbounded domains. *International Journal for Numerical Methods in Engineering* 2004; **59**(8): 1039–1074. DOI: 10.1002/nme.896.
27. Hallquist JO. LS-DYNA keyword user's manual, Livermore Software Technology Corporation 2016.
28. Lysmer J, Kuhlemeyer RL. Finite dynamic model for infinite media. *Journal of the Engineering Mechanics Division* 1969; **95**(4): 859–878.
29. Fenves G, Chopra AK. Effects of reservoir bottom absorption on earthquake response of concrete gravity dams. *Earthquake Engineering & Structural Dynamics* 1983; **11**(6): 809–829. DOI: 10.1002/eqe.4290110607.
30. Lotfi V, Roesset JM, Tassoulas JL. A technique for the analysis of the response of dams to earthquakes. *Earthquake Engineering & Structural Dynamics* 1987; **15**(4): 463–489. DOI: 10.1002/eqe.4290150405.

31. Bougacha S, Tassoulas JL. Seismic analysis of gravity dams. I: Modeling of sediments. *Journal of Engineering Mechanics* 1991; **117**(8): 1826–1837. DOI: 10.1061/(ASCE)0733-9399(1991)117:8(1826).
32. Zienkiewicz OC, Bettess P. Fluid-structure dynamic interaction and wave forces. An introduction to numerical treatment. *International Journal for Numerical Methods in Engineering* 1978; **13**(1): 1–16. DOI: 10.1002/nme.1620130102.
33. Bao H, Bielak J, Ghattas O, Kallivokas LF, O'Hallaron DR, Shewchuk JR, *et al.* Large-scale simulation of elastic wave propagation in heterogeneous media on parallel computers. *Computer Methods in Applied Mechanics and Engineering* 1998; **152**(1-2): 85–102. DOI: 10.1016/S0045-7825(97)00183-7.
34. Schnabel PB, Lysmer J, Seed HB. SHAKE: A computer program for earthquake response analysis of horizontally layered sites. *Report No. UCB/EERC-72/12*, Earthquake Engineering Research Center, Univ. of California, Berkeley: 1972.
35. Hashash YMA, Groholski DR, Phillips CA, Park D, Musgrove M. DEEPSOIL user manual and tutorial. Version 5.0, University of Illinois, Urbana, IL, USA 2011.
36. Joyner WB, Chen ATF. Calculation of nonlinear ground response in earthquakes. *Bulletin of the Seismological Society of America* 1975; **65**(5): 1315–1336.
37. Nielsen AH. Absorbing boundary conditions for seismic analysis in ABAQUS. *Proc. of the 2006 ABAQUS Users' Conference*, Boston, MA, USA: 2006.
38. Cundall PA, Coetzee MJ, Hart RD, Varona PM. FLAC user manual. Version 5.0, Itasca Consulting Group Inc., Minneapolis, MN, USA 1993.
39. McKenna F. OpenSees: A framework for earthquake engineering simulation. *Computing in Science and Engineering* 2011; **13**(4): 58–66. DOI: 10.1109/MCSE.2011.66.
40. Chopra AK. *Dynamics of Structures: Theory and Applications to Earthquake Engineering*. Upper Saddle River, NJ: Prentice Hall; 2012.
41. Fenves G, Chopra AK. EAGD-84: A computer program for earthquake analysis of concrete gravity dams. *Report No. UCB/EERC-84/11*, Earthquake Engineering Research Center, Univ. of California, Berkeley: 1984.
42. Mills-Bria B, Nuss L, Chopra AK. Current methodology at the Bureau of Reclamation for the nonlinear analyses of arch dams using explicit finite element techniques. *Proc. for 14th World Conference on Earthquake Engineering*, Beijing, China: 2008.
43. Curtis DD, Sooch G, Brewer T, Schildmeyer A. Explicit seismic analysis of Mossyrock Dam. *Proc. of the 33rd Annual USSD Conference*, Phenix, Arizona: 2013.